IEEE Access
Multidisciplinary | Rapid Review | Open Access Journal

Received July 23, 2018, accepted August 22, 2018, date of publication September 3, 2018, date of current version October 8, 2018.

Digital Object Identifier 10.1109/ACCESS.2018.2868197

Vibration Signal Prediction of Gearbox in High-Speed Train Based on Monitoring Data

YUMEI LIU[1], NINGGUO QIAO[1], CONGCONG ZHAO[2], AND JIAOJIAO ZHUANG[1]

[1]Transportation College, Jilin University, Changchun 130022, China
[2]The College of Engineering and Technology, Jilin Agricultural University, Changchun 130118, China

Corresponding authors: Yumei Liu (lymlls@163.com) and Ningguo Qiao (897516194@qq.com)

This work was supported in part by the National Natural Science Foundation of China under Grant 51575232 and in part by the National Science Foundation of Jilin Province, China, under Grant 20160204018GX.

ABSTRACT Vibration signals contain abundant information which can reflect the running state of high-speed trains. Accurate vibration signal prediction can provide references for anomaly detection of the gearbox in high-speed trains. This paper develops a hybrid model combining ensemble empirical mode decomposition (EEMD) with auto regression (AR) and support vector regression (SVR) models. First, the EEMD method is applied to decompose the vibration acceleration signal of gearbox. Second, AR models are employed to predict the intrinsic mode functions and the outputs are aggregated as the final result of AR. Third, reconstruct phase space and establish SVR models to predict the components; The predictions are aggregated as the final result of SVR. Finally, the results predicted using the AR and SVR models are weighted and summed together, with the weights being optimized by the chaotic particle swarm optimization algorithm. The actual operation monitoring data are used to validate the hybrid model. Data analysis demonstrates that the proposed method has better approximation compared with the AR model, the SVR model and the RBF neural network model.

INDEX TERMS High-speed train gearbox, vibration signal prediction, hybrid model, auto regression, support vector regression, chaotic particle swarm optimization.

I. INTRODUCTION

As an important component of high-speed train transmission system, gearbox is subjected to harsh conditions during actual operation. It not only bears the vibration transmitted by the body, but also is disturbed by the track irregularity. It consists of a pair of gear, a box, a shaft and four bearings. According to statistical analysis, the box and bearings are the most vulnerable components of the gearbox [1]. Once the failures occur, they will affect safe operation of the train, and even casualties. Therefore, accurate vibration signal prediction becomes more important for anomaly detection of gearbox.

The prediction of vibration signals is based on historical data and current monitoring data to predict the future trend, so that the abnormal vibration can be found as soon as possible. The approaches of modeling time series mainly utilize traditional models, intelligence technology and hybrid models [2].The traditional models are mainly based on statistical methods, such as the auto regression (AR) model, the autoregressive moving average (ARMA) model, and the autoregressive integrated moving average (ARIMA) model [3], [4]. These models are more suitable for stable time series. The AR model has the advantages of simple modeling and few parameters compared with others. In order to utilize the AR model to the non-stationary time series, Zhang *et al.* [5] proposed a method of differencing.

With the development of intelligence technology, artificial neural network (ANN) and support vector machine (SVM) have been widely applied in prediction field. Neural network is widely applied because of its strong nonlinear mapping ability and tolerance to noise. Reference [6] proposed a fault prognosis method using the adaptive fuzzy neural network to predict vibration trend of the rotating machinery. Yu decomposed the time series by wavelet and used the RBF neural network to predict different frequencies [7]. Li *et al.* [8] applied the neural network to forecast the vibration tendency of the aircraft engine. However, neural networks have some shortcomings, which need to train large number of samples. SVM can overcome the shortcomings of network effectively because it considers the sample error and the complexity in the modeling process. Lan proposed a method of using grid search to identify the parameters of SVM [9]. Gao and Li [10] proposed a method combining

phase space reconstruction with SVM for predicting the gyroscope drift time series. Reference [11] introduced the chaos theory into SVM and compared it with the neural network model.

Although intelligent technology is effective in dealing with nonlinear problems, they are not ideal to model the non-stationary data without preprocessing. Thus, combining signal processing with intelligent technology is an effective way to model nonlinear data sets. As a signal decomposition method, Empirical mode decomposition (EMD) has the advantage of self-adaptation. It can avoid the problem of choosing wavelet bases for wavelet decomposition. Thus, hybrid models combining EMD with SVR are studied in many researches. Duan *et al.* [12] developed a hybrid model of EMD-SVR to predict the non-stationary wave. Wang and Zhu [13] combined EMD with the Least Square Support Vector Machine (LS-SVM) model to predict vibration signal. Silva *et al.* [14] proposed a method combining EMD with the optimized SVM for forecasting the non-stationary time series. Because modal mixing phenomenon is easily appearing in the EMD method, Huang and Wu [15] proposed an improved method, that is, ensemble empirical mode decomposition (EEMD). Zhao developed a hybrid model combining EEMD with the AR model. The time series is first decomposed into several intrinsic mode functions (IMFs). Then, AR is employed to forecast the components individually, and the predictions of all components are aggregated to obtain the final result [16]. Zhang *et al.* [17] applied a hybrid model combining EEMD with the LSSVM-PSO model to forecast the time-varying time series. However, using a single model to predict the IMFs has its limitation. A single model is difficult to capture all the important features, especially for vibration signals of gearbox in high-speed trains. Due to the disturbance of track irregularities, the vibration signals are more complex. In view of this, we propose a hybrid model combining EEMD with the AR and SVR model, and the predictions are weighted and summed together to obtain the final result.

This work can be summarized as four steps: (1) the vibration acceleration of gearbox is collected when the train is running on the road, and the signal is decomposed by EEMD; (2) select the order and estimate the parameters of AR models. Use the AR models to predict IMFs and the predictions are summed to obtain the final result of AR; (3) determine the embedding dimension and establish SVR models to predict the components. The predictions are aggregated as the final result of SVR; (4) the results predicted using the AR and SVR models are weighted and summed together, with the weights being optimized by the chaotic particle swarm optimization (CPSO) algorithm.

The remaining sections of this paper are organized as follows. Section II outlines the theoretical basis of models. Section III constructs the hybrid model and gives the main steps of the method. Section IV is the experiment and data analysis. Section V presents our conclusions.

II. THEORETICAL METHODOLOGY

A. EEMD

Owing to the train track irregularity, the vibration signals of gearbox are nonlinear and non-stationary. Therefore, signal decomposition is required before prediction. There are many methods for data processing, Such as wavelet decomposition, EMD and EEMD. EEMD attracts us mainly because it is adaptive in analyzing nonlinear and non-stationary time series and can avoid modal mixing of EMD. The basic idea of EEMD is to add white noises into the results of EMD. The process of EEMD can be summarized as follows [18]–[22]:

1) Add a certain length of white noise $z(t)$ to the vibration signal $x(t)$ and obtain a composite signal $y(t) = x(t) + z(t)$;

2) Decompose $y(t)$ into a set of IMFs represented by c_j and a residual term represented by r;

$$y(t) = \sum_{j=1}^{J} c_j + r \tag{1}$$

3) Repeat step 1 and 2 with different amplitudes;

4) Take the mean of IMFs.

$$\begin{cases} \bar{c}_j = \dfrac{1}{M} \displaystyle\sum_{i=1}^{M} c_{i,j} \\ \bar{r}_j = \dfrac{1}{M} \displaystyle\sum_{i=1}^{M} r_i \end{cases} \quad (i = 1, 2, \ldots, M; j = 1, 2, \ldots, J) \tag{2}$$

where c_{ij} represents j-th IMF obtained by decomposition after adding i-th white noise; M is the number of aggregations; J is the number of IMFs; $\bar{c}_j$ is the mean of IMFs; and $\bar{r}_j$ represents the mean of the residual terms.

B. AUTO REGRESSION MODEL

Given the time series $x(t)$, the AR model is defined as (3)

$$x(t) = \sum_{k=1}^{n} \alpha_k x(t-k) + \omega(t) \tag{3}$$

where n represents the best order; $\alpha_u (u = 1, 2, \ldots, n)$ denotes the autoregressive coefficients; and $\omega(t)$ is a white noise sequence with zero mean and σ_{ω^2} variance.

We apply the AIC criterion to determine the order of the AR model [23].

$$AIC(n) = N \ln \sigma^2 + 2n \tag{4}$$

where σ^2 is the predictive variance; and N is the number of samples.

There are many kinds of methods to estimate the parameters of AR model, such as the Yule-Walker, the least squares, and the Burg algorithm [24], [25]. The Yule-Walker function is applied in this paper, and the specific process is expressed as follows [26].

Multiply $x(t-\tau)$ at the both ends of formula (3) and take average. The relation between the autocorrelation coefficients

and parameters can be obtained as in (5).

$$\begin{cases} R_x(\tau) + \sum_{i=1}^{n} \alpha_i R_x(\tau - i) = 0 & \tau = 1, 2, \ldots, n \\ R_x(\tau) + \sum_{i=1}^{n} \alpha_i R_x(\tau - i) = \delta^2 & \tau = 0 \end{cases} \tag{5}$$

where τ represents the time delay; and $R_x(\tau)$ represent the cross-correlation coefficients.

By rewriting (5) as a matrix form, we can obtain the Yule-Walker (Y-W) function

$$\begin{bmatrix} R(0) & R(-1) & \cdots & R(-n) \\ R(1) & R(0) & \cdots & R(1-n) \\ \vdots & \vdots & \cdots & \vdots \\ R(n) & R(n-1) & \cdots & R(0) \end{bmatrix} \begin{bmatrix} 1 \\ \alpha_1 \\ \vdots \\ \alpha_n \end{bmatrix} = \begin{bmatrix} \delta^2 \\ 0 \\ \vdots \\ 0 \end{bmatrix} \tag{6}$$

The autoregressive coefficients $\alpha_u (u = 1, 2, \ldots, n)$ are estimated using Levison-Durbin (L-D) algorithm.

C. SUPPORT VECTOR REGRESSION MODEL

The principle of SVR is to map the sample in the low-dimensional space R^l to the high-dimensional space H through the nonlinear mapping Φ, which is Φ: $R^l \to H$. The regression function is given in (7) [27], [28].

$$y = f(x) = \langle \omega, \Phi(x) \rangle + b (\Phi : R^l \to H) \tag{7}$$

where ω represents the weight vector and b is the bias.

To estimate the parameters ω and b, establish the following optimization problem.

$$\min(\omega) = \frac{1}{2} \|\omega\|^2 + C \sum_{i=1}^{l} \zeta (f(x_i) - y_i, x_i) \Gamma \tag{8}$$

where: $\sum_{i=1}^{l} \zeta(f(x_i) - y_i, x_i)$ represents the empirical risk term; $\frac{1}{2} \|\omega\|^2$ represents the regularization term; and the constant C is used to determine the trade-off between the two terms.

Utilize the sensitivity ε to measure the risk error to determine $\sum_{i=1}^{l} \zeta(f(x_i) - y_i, x_i)$.

$$\zeta (f(x) - y, x) = |y - f(x)|_\varepsilon = \begin{cases} 0 & |y - f(x)| \le \varepsilon \\ |y - f(x)| - \varepsilon & \text{else} \end{cases} \tag{9}$$

Introduce the slack variables ξ_i and ξ_i^* to (8) and rewrite it as (10).

$$\min \Gamma(\omega) = \frac{1}{2} \|\omega\|^2 + C \sum_{i=1}^{l} (\zeta_i + \zeta_i^*) \tag{10}$$

$$s.t. \ \langle \omega, \Phi(x_i) \rangle + b - y_i \le \zeta_i + \varepsilon$$
$$y_i - \langle \omega, \Phi(x_i) \rangle - b \le \zeta_i^* + \varepsilon$$
$$\zeta_i, \zeta_i^* \ge 0, \quad i = 1, 2, \ldots, l \tag{11}$$

Add the Lagrange multipliers $\alpha_i^{(*)}$ and $\eta_i^{(*)}$ to (10)

$$\begin{aligned} L(\omega, b, \zeta_i^*) = {} & \frac{1}{2} \|\omega\|^2 - \sum_{i=1}^{l} \alpha_i (\varepsilon + \zeta_i + y_i - \langle \omega, \Phi(x_i) \rangle - b) \\ & + C \sum_{i=1}^{l} (\zeta_i + \zeta_i^*) \\ & - \sum_{i=1}^{l} \alpha_i^* (\varepsilon + \zeta_i^* - y_i + \langle \omega, \Phi(x_i) \rangle + b) \\ & - \sum_{i=1}^{l} (\eta_i \zeta_i + \eta_i^* \zeta_i^*) \end{aligned} \tag{12}$$

where $\alpha_i^{(*)}$ and b are obtained by computing (13),

$$\begin{aligned} & \min W(\alpha_i^{(*)}) \\ & = \frac{1}{2} \sum_{i,j=1}^{l} (\alpha_i^* - \alpha_i)(\alpha_j^* - \alpha_j) \langle \Phi(x_i), \Phi(x_j) \rangle \\ & \quad + \varepsilon \sum_{i=1}^{l} (\alpha_i^* + \alpha_i) - \sum_{i=1}^{l} y_i (\alpha_i^* - \alpha_i) \end{aligned} \tag{13}$$

$$\begin{aligned} & s.t. \sum_{i=1}^{l} (\alpha_i^* - \alpha_i) = 0 \\ & 0 \le \alpha_i \le C \\ & 0 \le \alpha_i^* \le C \end{aligned} \tag{14}$$

We can obtain (15) by solving (13).

$$f(x) = \sum_{i=1}^{l} (\alpha_i^* - \alpha_i) K(x_i, x) - b \tag{15}$$

where $K(x_i, x)$ represents the RBF kernel function, which is expressed as

$$K(x_i, x_j) = \exp\left(-\gamma \|x_i - x_j\|^2\right) \quad \gamma > 0 \tag{16}$$

where γ represents the parameter of RBF function.

D. PHASE SPACE RECONSTRUCTION

For a set of time series $X_N = (x_1, x_2, \ldots, x_N)$, use the known data before t moment to predict the data of $t + 1$ moment. We can construct a mapping like (17):

$$\hat{x}_{t+1} = f(x_t, x_{t-1}, \ldots, x_{t-(m-1)}) \tag{17}$$

where m represents the embedding dimension.

Transform (17) into a matrix.

$$\begin{aligned} X &= \begin{bmatrix} \bar{x}_{m+1} \\ \bar{x}_{m+2} \\ \vdots \\ \bar{x}_N \end{bmatrix} = \begin{bmatrix} x_1 & x_2 & \cdots & x_m \\ x_2 & x_3 & \cdots & x_{m+1} \\ \vdots & \vdots & \cdots & \vdots \\ x_{N-m} & x_{N-m+1} & \cdots & x_{N-1} \end{bmatrix}, \\ Y &= \begin{bmatrix} x_{m+1} \\ x_{m+2} \\ \vdots \\ x_N \end{bmatrix} \end{aligned} \tag{18}$$

The predictive errors of the SVR model are evaluated by the final prediction criterion (FPE). The minimum of FPE is used to determine the best embedding dimension m. The functions are described in (19) and (20).

$$FPE\ (m) = \frac{N+m}{N-m}\sigma_\alpha^2 \tag{19}$$

$$\sigma_\alpha^2 = E\left(\alpha_{n_N}\right) = \frac{1}{N-m} \times \sum_{t=m+1}^{N}\left[x_t - \left(\sum_{i=1}^{N=m}\left(\left(\alpha_i^* - \alpha_i\right)K\left(x_i, x_t\right)\right) + b\right)\right]^2 \tag{20}$$

The regression equation after phase space reconstruction is expressed as (21):

$$x_{t+1} = f\left(\bar{x}_t\right) = \sum_{i=1}^{N-m}\left(\alpha_i^* - \alpha_i\right)K\left(\bar{x}_i, \bar{x}_t\right) + b \quad (t = m+1, m+2, \ldots N) \tag{21}$$

So one-step prediction of the SVR model is obtained.

$$\hat{x}_{N+1} = \sum_{i=1}^{N-m}\left(\alpha_i^* - \alpha_i\right)K\left(\bar{x}_i, \bar{x}_{N+1}\right) + b \tag{22}$$

where $\bar{x}_{N+1} = \{x_{N-m+1}, x_{N-m+2}, \ldots, x_N\}$, and $\hat{x}_{N+1}$ is the predictive value of the $N+1$ point.

The iteration method is used to obtain the predictive value of the l step.

$$\hat{x}_{N+l} = \sum_{i=1}^{N-m}\left(\alpha_i^* - \alpha_i\right)K\left(\bar{x}_i, \bar{x}_{N+L}\right) + b \tag{23}$$

III. CONSTRUCT THE HYBRID MODEL

A. CONSTRUCT THE EEMD-AR-SVR-CPSO MODEL

To take full advantage of the nonlinear and linear characteristics of the SVR and AR models, a hybrid model of EEMD-AR-SVR-CPSO is constructed. The flowchart is presented in Fig. 1 and the specific steps are described as follows:

1) Vibration acceleration signals of the gearbox in high-speed train are collected;

2) Pre-process the signal using EEMD to obtain a set of IMFs;

3) Calculate the autocorrelation coefficients of the time series X_N and solve the *Y-W* equation using *L-D* algorithm;

4) The minimum AIC value is chosen as the optimal order;

5) The AR model is constructed to predict the IMFs, and the predictions are summed as the result of AR represented by y_1;

6) Reconstruct phase space for the vibration signal time series;

7) Use grid search method to optimize parameters C and γ;

8) Determine the optimum embedding dimension m according to *FPE* criterion;

9) SVR models are constructed to predict IMFs, and the predictions of IMFs are summed as the result of SVR represented by y_2;

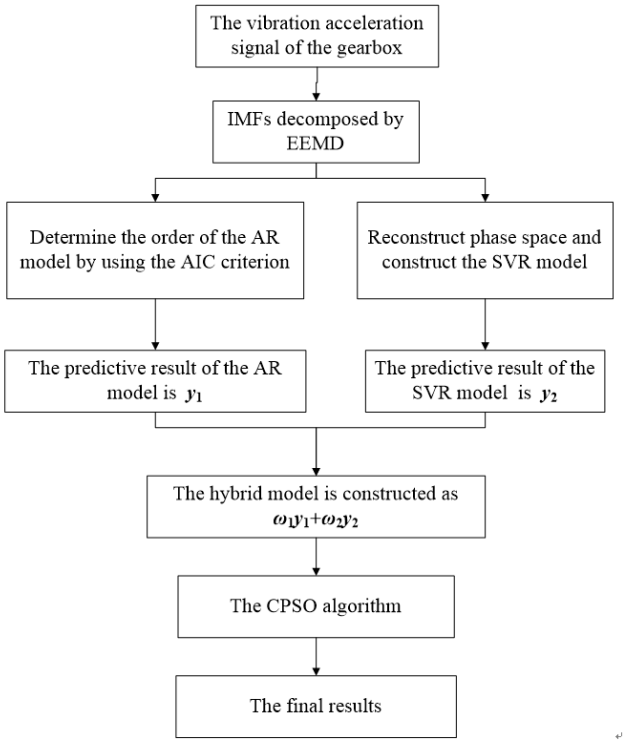

FIGURE 1. The frame of the hybrid model.

10) Construct a linear combination $\omega_1 y_1 + \omega_2 y_2$, and use the CPSO to determine the weights of the AR and SVR in the hybrid model;

B. CHOTIC PARTICLE SWARM OPTIMIZATION

PSO is a method to find the optimum solution, which shows obvious advantages in solving complex problems. The core of PSO is to optimize the population by updating their extremes. The specific process is expressed as follows [29]–[33].

Assume that the velocity and position of u-th particle in the e dimensional space are $v_u = (v_{u1}, v_{u2}, \ldots, v_{ue})^T$ and $x_u = (x_{u1}, x_{u2}, \ldots, x_{ue})^T$. The best historical positions of u-th particle in the populations are $p_u = (p_{u1}, p_{u2}, \ldots, p_{ue})$ and $p_g = \left(p_{g1}, p_{g2}, \ldots, p_{ge}\right)$. Update the velocity and position using (24),

$$\begin{cases} v_{ue}^{(l+1)} = \omega^{(l+1)} v_{ue}^{(l)} + \alpha_1 r_1 (p_{ue}^{(l)} - X_{ue}^{(l)}) + \alpha_2 r_2 (p_{ge}^{(l)} - X_{ue}^{(l)}) \\ X_{ue}^{(l+1)} = X_{ue}^{(l)} + v_{ue}^{(l+1)} \quad (u = 1, 2, \ldots, h;\ e = 1, 2, \ldots E) \end{cases} \tag{24}$$

where l are the iteration times; $v_{ue}^{(l)}$ is the velocity of u-th particle at l-th iteration; $X_{ue}^{(l)}$ is the position of u-th particle at l-th iteration; h is the particle number; E is the particle dimension; α_1 and α_2 are the acceleration factors with the values ranging from 1 to 2; r_1 and r_2 are random numbers; and $\omega^{(l)}$ is the inertia weight, whose expression is described

as (25).

$$\omega^{(l)} = \frac{t}{T_{\max}}\left(\omega_{fin} - \omega_{ini}\right) + \omega_{ini} \tag{25}$$

where ω_{ini} represents the initial weight; ω_{fin} represents the final weight; $T_{\max}$ represents the maximum iterations; and t represents the current iteration.

As an improved algorithm, CPSO introduces the chaos theory into PSO. It can effectively overcome the shortcomings of PSO. Logistic equation is a typical chaotic equation, which can be used to generate chaotic variables. The iteration of Logistics is expressed as (26).

$$x_{n+1} = \mu x_n(1 - x_n) \tag{26}$$

where μ represents the control parameter. When $\mu = 4$ and $x_n \in [0,\ 1]$, the Logistic system is a complete chaotic system, throughout the interval of [0, 1].

The specific steps of the CPSO algorithm are summarized as follows [34]:

1) Initialize the population;

2) Update v_u and x_u using (24) and calculate the fitness value;

3) The global optimum position generated at l-th iteration is processed using (27) and mapped to the interval of [0, 1]:

$$z_u^l = \frac{p_{gu}^{(l)} - a_u^{(l)}}{b_u^{(l)} - a_u^{(l)}} \tag{27}$$

where $a_u^{(l)}$ and $b_u^{(l)}$ represent the lower and upper limit of the feasible search space at l-th iteration;

4) Iterate N_q times on $z_u^{(l)}$ and generate the chaotic sequences $z_{um}^{(l)}(m = 1, 2, \ldots, N_q)$;

5) Return the generated chaotic sequence $z_{um}^{(l)}(m = 1, 2, \ldots, N_q)$ to the original solution space using (28) and obtain a feasible solution containing chaotic variables $p_{gu,m}^{(*l)} = \left(p_{g1,m}^{(*l)}, p_{g2,m}^{(*l)}, \ldots, p_{gh,m}^{(*l)}\right)$;

$$p_{gu,m}^{(*l)} = a_u^{(l)} + \left(b_u^{(l)} - a_u^{(l)}\right) z_{u,m}^{(l)} \quad (m = 1, 2, \ldots, N_q;\ u = 1, 2, \ldots, h) \tag{28}$$

where $p_{gu,m}^{(l)}$ represents m-th chaotic sequence;

6) Calculate the fitness values of each feasible solution $p_{gu,m}^{(*)}$ and obtain the optimal feasible solution $p_g^{(*l)}$;

7) Judge whether $p_g^{(*l)}$ is the current optimal solution. If $p_g^{(*l)}$ is better than the current optimum location $p_g^{(l)}$ or the chaotic search reaches the maximum steps, then the chaotic search iterations can be stopped, otherwise $m = m + 1$;

8) Update the extreme values of individuals and populations. If they have satisfied the termination condition, the iteration can be finished; Otherwise, go to step 9;

9) Contract the feasible search region and generate the remaining particles as in (29), then go to step 2.

$$\begin{cases} a_u^{(l)} = \max\left(a_u^{(l)}, p_u^{(l)} - \gamma \times \left(b_u^{(l)} - a_u^{(l)}\right)\right) \\ b_u^{(l)} = \min\left(b_u^{(l)}, p_u^{(l)} + \gamma \times \left(b_u^{(l)} - a_u^{(l)}\right)\right) \end{cases} \tag{29}$$

where $p_u^{(l)}$ represents the best individual at l-th iteration;

C. THE FITNESS FUNCTION OF CPSO

The square sum of prediction errors is defined as the fitness function of CPSO. The specific process is given in (30) and (31).

$$f = \min \sigma^2 = \min \sum_{i=1}^{N} (\omega_1 y_1(i) + \omega_2 y_2(i) - x_i)^2 \tag{30}$$

$$s.t.\ \omega_1 + \omega_2 = 1$$
$$\omega_1 \geq 0, \quad \omega_2 \geq 0 \tag{31}$$

IV. DATA ANALYSIS

A. DATA SETS

Signals were collected by China CNR Corporation Limited. The sampling interval is Harbin to Dalian in China [35]. Signals are collected by the LMS digital acquisition system and the sampling frequency is 2048Hz. The type of sensors is UL2017 and the vibration measuring point is shown in Fig.2. Vertical, longitudinal, and transverse vibration accelerations are measured in the test. But in this paper, only the vertical

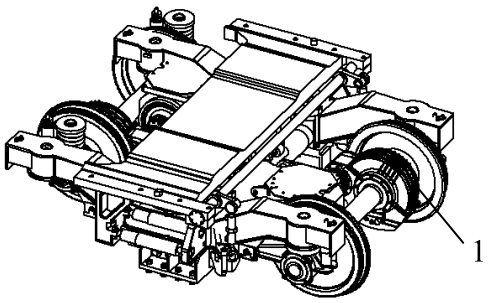

FIGURE 2. The installation position of the sensor.

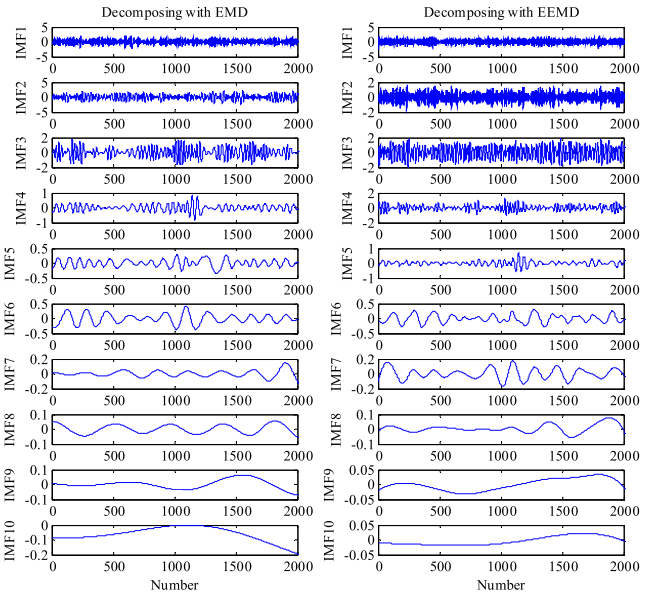

FIGURE 3. The decomposition results with EMD and EEMD.

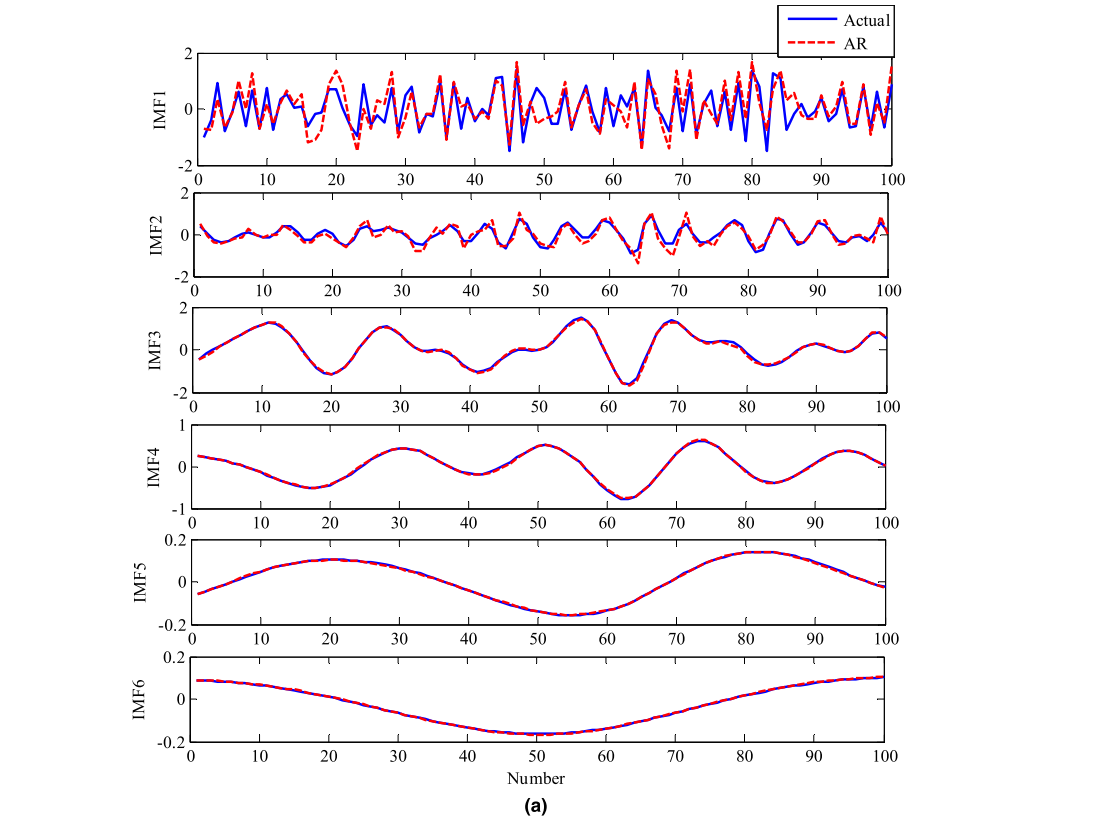

FIGURE 4. (a) The predictive results of the IMFs with the AR model (b) The prediction of the signal after EEMD and (c) the prediction of the original signal with AR models.

vibration acceleration is employed to verify the effectiveness of the method. Take 200 minutes vibration signals as the training data and 10 points per minute.

B. SIGNAL PRE-PROCESSING

Due to the disturbance of track irregularity, there is a lot of noise in the collected signal. Performing EEMD and EMD on the signal, and the decomposition results are presented in Fig.3. The added white noise has amplitude of 0.2 standard deviation of the signal, and the ensemble size is 100 [36]. From Fig.3, it could be seen that the signal is decomposed into 10 IMFs. By comparison, the phenomenon of mode mixing occurs from IMF2 to IMF7 with EMD method. Instead, EEMD overcomes this problem. Since there is little effective information contained in the latter IMF components, we only predict and aggregate the first 6 IMFs.

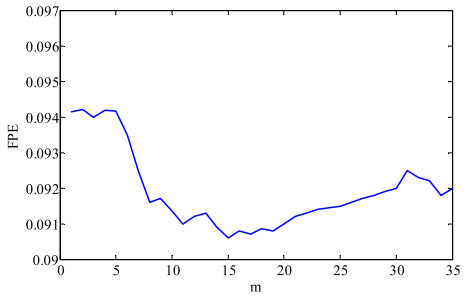

FIGURE 5. The distribution of FPE.

C. THE PREDICTION OF AR MODEL

The determination of order and estimation of parameters are two important problems of the AR model. The initial order is defined with $n = \sqrt{2000} \approx 45$ and the best order n is determined using (4). The autoregressive coefficients

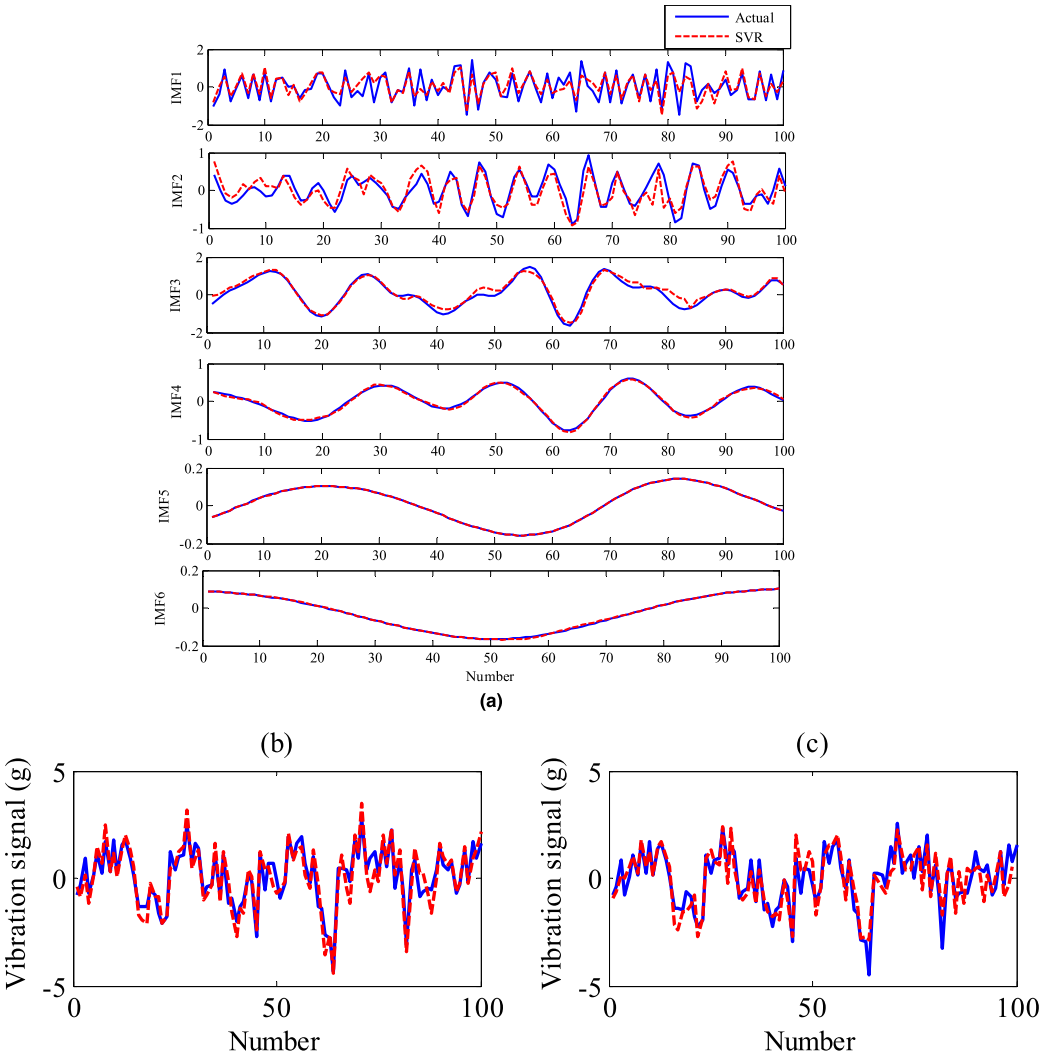

FIGURE 6. (a) The predictions of the IMFs with the SVR model (b) the prediction of the signal after EEMD and (c) the prediction of the original signal with SVR models.

α_u $(u = 1, 2, \ldots, n)$ and the white noise sequence $\omega(t)$ are obtained by constructing the Y-W equation and using L-D iteration algorithm. On these bases, IMFs are predicted respectively shown in Fig. 4(a). We can find that there are some deviations in the prediction of high-frequency components using the AR model, while the ability to approximate the low-frequency part is stronger. The predictions of IMFs are summed as shown in Fig. 4(b). By comparing the advantages of the prediction after decomposition, we model the original vibration time series directly. From the results of Figs. 4(b) and 4(c), we can draw a conclusion that the prediction accuracy of the signal after decomposition is higher.

D. THE PREDICTION OF THE SVR MODEL

Use 2000 data to train SVR models and the optimal embedding dimension is determined using (19) and (20). The FPE values vary with the embedding dimension m is shown in Fig.5. The optimal embedding dimension $m = 15$ and the minimum of FPE is 5.071×10^3. Parameters C and γ are optimized with the grid search method and the predictive results are shown in Fig.6.

By analyzing Figs.4 and 6, the conclusion is drawn that the SVR model has better nonlinear approximation ability than the AR model. Moreover, the prediction accuracy after EEMD is higher than that of the original signal. However, the predictions of the AR and SVR models deviate from the real values at different points, and the errors are mainly due to their own limitations. Therefore, we can combine the two models.

E. THE PREDICTION OF THE HYBRID MODEL

The hybrid model of EEMD-AR-SVR-CPSO was constructed and the fitness function of the CPSO algorithm was determined. The parameters of CPSO are set as follows: the learning factors are $c_1 = c_2 = 1.496$; the number of particles is 50; the initial weight $\omega_{ini} = 0.9$ and the termination weight

$\omega_{fin} = 0.4$; and the iterations number is $N_q = 200$. To verify the superiority of CPSO, the PSO algorithm is also used to optimize the target function, and the parameters are set the same as CPSO. The fitness curves are shown in Fig.7, where the CPSO algorithm converges faster than the PSO. The CPSO converges at the 27 iterations, while the PSO converges at the 73 iterations.

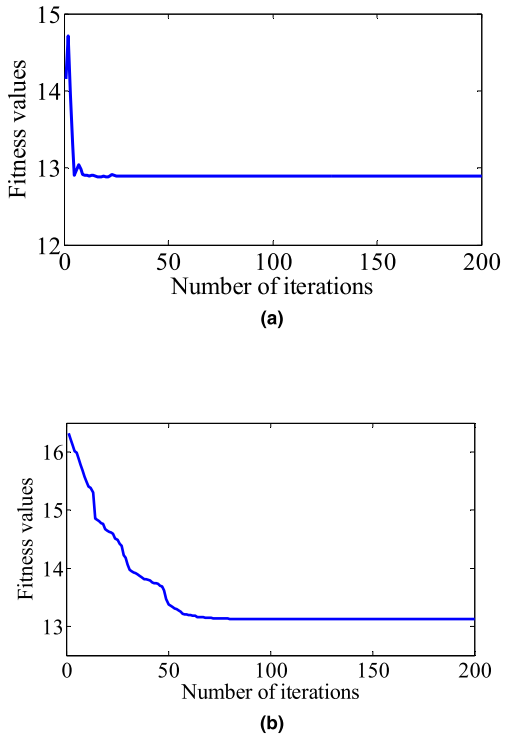

FIGURE 7. The fitness curves. (a) CPSO algorithm. (b) PSO algorithm.

Through optimization, the weight of AR in the hybrid model is $\omega_1 = 0.4265$, and the weight of SVR in the hybrid model is $\omega_2 = 0.5735$. The hybrid model is thus determined as (32). As shown in Fig.8, the hybrid model can well approximate the true values and has good prediction performance.

$$Y = 0.4265y_1 + 0.5735y_2 \tag{32}$$

F. THE PREDICTION OF THE RBF NEURAL NETWORK MODEL

The RBF neural network model was established to make the comparison with the SVR model. The RBF neural network (RBFNN) chooses three-layers. With the embedding dimension $m = 15$, the number of inputs is 15, and the number of outputs is 1. The transfer function of the hidden layer is the 'radbas', and the transfer function of the output layer is the 'purelin'. In addition, the spread of RBF exerts great influence on the performance of the network. Through training, the spread was determined as 0.24 [37]. From Fig. 9(a), we can see that the prediction of the RBF neural network model has deviations at the inflection points for high-frequency components, but the approximation performance to the low-frequency components is good.

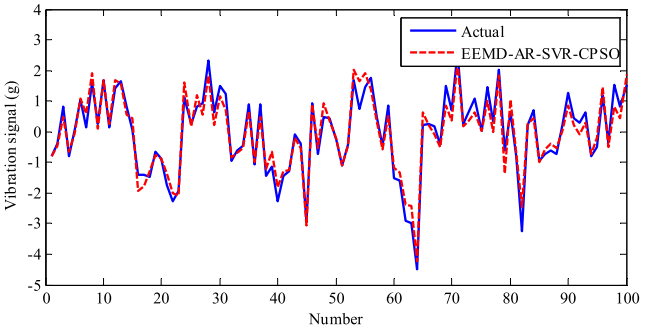

FIGURE 8. The prediction of the EEMD-AR-SVR-CPSO model.

Furthermore, the EEMD-AR-RBFNN-CPSO hybrid model was also established to train and predict the vibration signal, and the weights are optimized as $\omega_1 = 0.5658$, $\omega_2 = 0.4342$. Compared with Figs. 9(b) and 9(d), the EEMD-AR-RBFNN-CPSO hybrid model has better nonlinear approximation ability than the EEMD-RBFNN model.

G. THE EVALUATION OF MODELS

To evaluate the prediction performance of models intuitively, we choose the following indexes. Assuming that measured data are $y = \{y_1, y_2, \ldots y_N\}$ and the predictive values are $\hat{y} = \{\hat{y}_1, \hat{y}_2, \ldots \hat{y}_N\}$, then the indexes are defined as follows [38] and [39]:

Mean absolute error (MAE):

$$MAE = \frac{1}{N}\sum_{i=1}^{N}\left|\frac{y_i - \hat{y}_i}{y_i}\right| \times 100\% \quad (i = 1, 2, \ldots, N) \tag{33}$$

Root mean square error (RMSE):

$$RMSE = \sqrt{\frac{1}{N}\sum_{i=1}^{N}\left(\frac{y_i - \hat{y}_i}{y_i}\right)^2} \quad (i = 1, 2, \ldots, N) \tag{34}$$

By using the absolute values, the MAE can avoid the offset of the positive and negative terms effectively and can better reflect the prediction deviations. RMSE shows the approximation ability of the models. The smaller the value, the better the predicted data are approximated to the true values.

We first consider the single prediction models. As shown in table 1, the SVR model has the better performance than the AR model, which explains that the vibration signal contains nonlinear characteristics. In addition, under the small

TABLE 1. Prediction errors of models.

models	MAE (%)	RMSE
The AR model	11.41	1.4043
The EEMD-AR model	6.62	0.8133
The SVR model	6.59	0.8256
The EEMD-SVR model	4.99	0.6304
The EEMD-AR-SVR-CPSO	2.66	0.3269
The EEMD-RBFNN	6.99	0.6918
The EEMD-AR-RBFNN-CPSO	4.18	0.5016

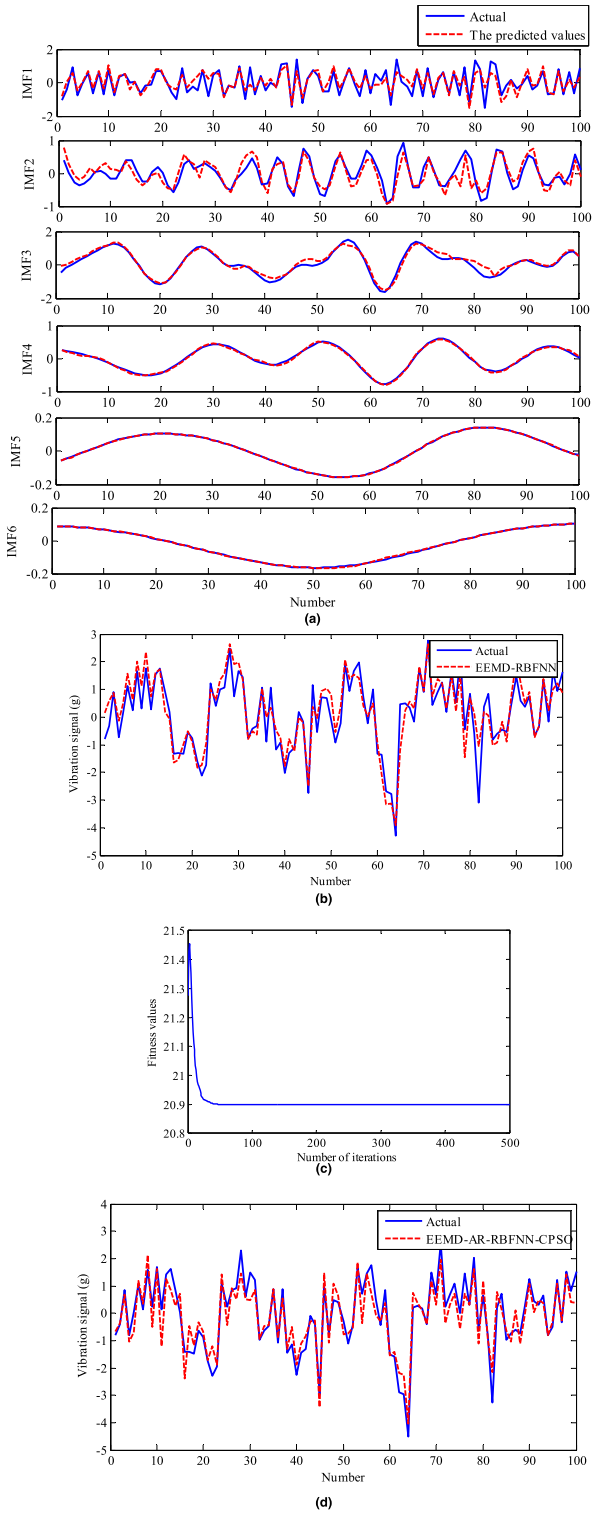

FIGURE 9. The predictions with the RBF neural network. (a) The predictions of the IMFs with the RBF neural network. (b) The final result of the vibration signal after EEMD with the RBF neural network. (c) The fitness curves. (d) The prediction of the EEMD-AR-RBFNN-CPSO model.

sample scale, the SVR model has higher fitting accuracy than the neural network model. When comparing hybrid models, obviously, the prediction accuracy after EEMD is improved. The RMSE of EEMD-AR model is 0.591 higher than that of the AR model. The RMSE of EEMD-SVR model is 0.1952 higher than that of the SVR model. Besides, The EEMD-SVR model is better than the EEMD-AR model. The RMSE of the EEMD-SVR model is 0.1829 higher than that of the EEMD-AR model, and 0.0614 higher than that of the EEMD-RBFNN model. Moreover, the EEMD-AR-SVR-CPSO model has the best performance. The absolute error is 1.52% higher than the EEMD-AR-RBFNN-CPSO model and the RMSE is the minimum.

V. CONCLUSION

This work addresses a hybrid model which is called EEMD-AR-SVR-CPSO to predict the vibration signal of gearbox in high-speed train for the first time. The goal of this work is to provide references for anomaly detection of gearbox. We take the advantage of AR modeling and the ability of SVR processing nonlinear time-series. Through collection and analysis of the experimental data, we can get the following two conclusions:

1) Whether the AR model or the SVR model, the precision predicted after EEMD is higher than that of the original signal. Under the small sample size, the precision of the SVR is higher than that of the RBF neural network. The EEMD-AR-SVR-CPSO model has the better performance by comparing with the AR model, the SVR model, and the RBF neural network model.

2) In view of time cost, it takes the shortest time to predict the original signal directly. After the signal is preprocessed, the time taken is almost 2∼3 times that of the original signal.

Future studies should focus on finding new models to improve the prediction efficiency to meet the real-time requirements. Another work is to use multi-step predictive data to evaluate the running state of gearbox in high-speed trains [40]–[45].

REFERENCES

[1] C. C. Zhao, "Analysis and evaluation of reliability for high-speed train transmission system," M.S. thesis, Transp. College, Jilin Univ., Changchun, China, 2016.

[2] X. Jiang, L. Zhang, and X. Chen, "Short-term forecasting of high-speed rail demand: A hybrid approach combining ensemble empirical mode decomposition and gray support vector machine with real-world applications in China," *Transport. Res. C, Emerg. Technol.*, vol. 44, no. 4, pp. 110–127, 2014.

[3] Z. Zhao *et al.*, "LSTM network: A deep learning approach for short-term traffic forecast," *IET Intell. Transp. Syst.*, vol. 11, no. 2, pp. 68–75, 2017.

[4] S. Dindarloo, "Reliability forecasting of a load-haul-dump machine: A comparative study of ARIMA and neural networks," *Qual. Rel. Eng. Int.*, vol. 32, no. 4, pp. 1545–1552, 2016.

[5] Q. Zhang, B.-D. Wang, B. He, Y. Peng, and M.-L. Ren, "Singular spectrum analysis and ARIMA hybrid model for annual runoff forecasting," *Water Resour. Manage.*, vol. 25, no. 11, pp. 2683–2703, 2011.

[6] D. Zurita-Millan *et al.*, "Vibration signal forecasting on rotating machinery by means of signal decomposition and neurofuzzy modeling," *Shock Vib.*, vol. 2016, pp. 1–13, Jul. 2016.

[7] W. Yu, J. Su, and W. Zhang, "Research on short-term traffic flow prediction based on wavelet de-noising preprocessing," in *Proc. 9th Int. Conf. Natural Comput.*, 2013, pp. 252–256.

[8] F. X. Li *et al.*, "Hybrid prediction method based on empirical mode decomposition and RBF neural network," *J. Vib. Meas. Diag.*, vol. 32, no. 5, pp. 817–822, 2012.

[9] Y. Y. Lan, "Forecasting performance of support vector machine for the Poyang Lake's water level," *Water. Sci. Technol.*, vol. 70, no. 9, pp. 1488–1495, 2014.
[10] Y. H. Gao and Y. B. Li, "Fault prediction model based on phase space reconstruction and least squares support vector machines," in *Proc. 9th Int. Conf. Hybrid Intell. Syst.*, vol. 3, Aug. 2009, pp. 464–467.
[11] F. Huang, J. Huang, S.-H. Jiang, and C. Zhou, "Prediction of groundwater levels using evidence of chaos and support vector machine," *J. Hydroinform.*, vol. 19, no. 4, pp. 586–606, 2017.
[12] W. Y. Duan, Y. Han, L. M. Huang, B. B. Zhaoa, and M. H. Wang, "A hybrid EMD-SVR model for the short-term prediction of significant wave height," *Ocean. Eng.*, vol. 124, pp. 54–73, Sep. 2016.
[13] H.-B. Wang and Q.-B. Zhu, "Trend prediction of non-stationary vibration signals based on empirical mode decomposition and least square support vector machine," *Comput. Eng. Appl.*, vol. 44, no. 16, pp. 157–159, 2008.
[14] I. D. da Silva, M. das Chagas Moura, I. D. Lins, E. L. Droguett, and E. Braga, "Non-stationary demand forecasting based on empirical mode decomposition and support vector machines," *IEEE Latin Amer. Trans.*, vol. 15, no. 9, pp. 1785–1792, Aug. 2017.
[15] N. E. Huang and Z. Wu, "A review on Hilbert–Huang transform: Method and its applications to geophysical studies," *Rev. Geophys.*, vol. 46, no. 2, p. RG2006, 2008.
[16] X.-H. Zhao and X. Chen, "Auto regressive and ensemble empirical mode decomposition hybrid model for annual runoff forecasting," *Water. Resour. Manage.*, vol. 29, no. 8, pp. 2913–2926, 2015.
[17] J.-L. Zhang, Y.-J. Zhang, and L. Zhang, "A novel hybrid method for crude oil price forecasting," *Energy Econ.*, vol. 49, pp. 649–659, May 2015.
[18] X. Kong *et al.*, "Mobility dataset generation for vehicular social networks based on floating car data," *IEEE Trans. Veh. Technol.*, vol. 67, no. 5, pp. 3874–3886, May 2018.
[19] X. Kong, X. Song, F. Xia, H. Guo, J. Wang, and A. Tolba, "LoTAD: Long-term traffic anomaly detection based on crowdsourced bus trajectory data," *World Wide Web*, vol. 21, no. 3, pp. 825–847, 2018.
[20] W. C. Wang, D. M. Xu, K. W. Chau, and S. Chen, "Improved annual rainfall-runoff forecasting using PSO-SVM model based on EEMD," *J. Hydroinform.*, vol. 15, no. 4, pp. 1377–1390, 2013.
[21] A. Rahim *et al.*, "Vehicular social networks: A survey," *Pervasive Mobile Comput.*, vol. 43, pp. 96–113, Jan. 2018.
[22] Y.-M. Liu, C.-C. Zhao, M.-Y. Xiong, Y.-H. Zhao, N.-G. Qiao, and G.-D. Tian, "Assessment of bearing performance degradation via extension and EEMD combined approach," *J. Central South Univ.*, vol. 24, no. 5, pp. 1155–1163, 2017.
[23] M. T. Zhu and J. Liu, "Research on method of determining order of AR model for road roughness reconstruction," *J. Highway Transp. Res. Develop.*, vol. 27, no. 7, pp. 25–28, 2010.
[24] N. Zhao, Q. Xu, and H. Wang, "Marginal screening for partial least squares regression," *IEEE Access*, vol. 5, pp. 14047–14055, 2017.
[25] G. Tian, H. Zhang, M. Zhou, and Z. Li, "AHP, gray correlation, and TOPSIS combined approach to green performance evaluation of design alternatives," *IEEE Trans. Syst., Man, Cybern., Syst.*, vol. 48, no. 7, pp. 1093–1105, Jul. 2018.
[26] M. Kallas, P. Honeine, C. Francis, and H. Amoud, "Kernel autoregressive models using Yule–Walker equations," *Signal Process.*, vol. 93, no. 11, pp. 3053–3061, 2013.
[27] X. K. Wei *et al.*, "Analysis and applications of time series forecasting model via support vector machines," *Syst. Eng. Electron.*, vol. 27, no. 3, pp. 529–532, 2005.
[28] S. Dong and T. Luo, "Bearing degradation process prediction based on the PCA and optimized LS-SVM model," *Measurement*, vol. 46, no. 9, pp. 3143–3152, 2013.
[29] X. Zhang, K. Song, C. Li, and L. Yang, "Parameter estimation for multi-scale multi-lag underwater acoustic channels based on modified particle swarm optimization algorithm," *IEEE Access*, vol. 5, pp. 4808–4820, 2017.
[30] G. Tian, M. Zhou, and P. Li, "Disassembly sequence planning considering fuzzy component quality and varying operational cost," *IEEE Trans. Autom. Sci. Eng.*, vol. 15, no. 2, pp. 748–760, Apr. 2018.
[31] R.-I. Chang, H.-M. Hsu, S.-Y. Lin, C.-C. Chang, and J.-M. Ho, "Query-based learning for dynamic particle swarm optimization," *IEEE Access*, vol. 5, pp. 7648–7658, 2017.
[32] Y. Zhou, N. Wang, and W. Xiang, "Clustering hierarchy protocol in wireless sensor networks using an improved PSO algorithm," *IEEE Access*, vol. 5, pp. 2241–2253, 2017.
[33] H. Y. Xiong, X. L. Zhu, and R. H. Zhang, "Energy recovery strategy numerical simulation for dual axle drive pure electric vehicle based on motor loss model and big data calculation," *Complexity*, vol. 2018, 2018, Art. no. 4071743, doi: 10.1155/2018/4071743.
[34] Y. Cheng *et al.*, "Structural reliability optimal design based on chaos particle swarm optimization," *J. Central South Univ.*, vol. 42, no. 3, pp. 671–676, 2011.
[35] F. Wang, X. Li, B. Zhang, and X.-Y. Wang, "A study on time series models and criterion rules based on condition monitoring of the tracking test system," in *Proc. Int. Conf. Mechatronic Sci., Electr. Eng. Comput.*, 2014, pp. 663–667.
[36] Z. Wu and N. E. Huang, "Ensemble empirical mode decomposition: A noise-assisted data analysis method," *Adv. Adapt. Data Anal.*, vol. 1, no. 1, pp. 1–41, 2008.
[37] M. Awad, "Forecasting of chaotic time series using RBF neural networks optimized by genetic algorithms," *Int. Arab Inf. Technol.*, vol. 14, no. 6, pp. 826–834, 2017.
[38] G. Tian *et al.*, "Operation patterns analysis of automotive components remanufacturing industry development in China," *J. Cleaner Prod.*, vol. 164, pp. 1363–1375, Oct. 2017.
[39] D. Wang, K.-L. Tsui, and Q. Miao, "Prognostics and health management: A review of vibration based bearing and gear health indicators," *IEEE Access*, vol. 6, pp. 665–676, 2018.
[40] X. J. Sun, H. Zhang, W. J. Meng, R. H. Zhang, K. L. Li, and T. Peng, "Primary resonance analysis and vibration suppression for the harmonically excited nonlinear suspension system using a pair of symmetric viscoelastic buffers," *Nonlinear Dyn.*, vol. 94, no. 4, pp. 1–23, 2018, doi: 10.1007/s11071-018-4421-9.
[41] R.-H. Zhang, Z.-C. He, H.-W. Wang, F. You, and K.-N. Li, "Study on self-tuning tyre friction control for developing main-servo loop integrated chassis control system," *IEEE Access*, vol. 5, pp. 6649–6660, 2017.
[42] S. Zhao, V. Makis, S. Chen, and Y. Li, "Evaluation of reliability function and mean residual life for degrading systems subject to condition monitoring and random failure," *IEEE Trans. Rel.*, vol. 67, no. 1, pp. 13–25, Mar. 2018.
[43] A. Rai and S. H. Upadhyay, "Bearing performance degradation assessment based on a combination of empirical mode decomposition and k-medoids clustering," *Mech. Syst. Signal Process.*, vol. 93, pp. 16–29, Sep. 2017.
[44] W. Ahmad, S. A. Khan, and J.-M. Kim, "A hybrid prognostics technique for rolling element bearings using adaptive predictive models," *IEEE Trans. Ind. Electron.*, vol. 65, no. 2, pp. 1577–1584, Feb. 2018.
[45] Y. Qi, C. Shen, D. Wang, J. Shi, X. Jiang, and Z. Zhu, "Stacked sparse autoencoder-based deep network for fault diagnosis of rotating machinery," *IEEE Access*, vol. 5, pp. 15066–15079, Jul. 2017.

YUMEI LIU received the Ph.D. degree from Jilin University, Changchun, China, in 2006. In 2007, she was a Visiting Scholar with the University of Bath, where she was appointed as a Guest Professor. She is currently a Professor at Transportation College, Jilin University. She has hosted two projects supported by the National Science and Technology Support Program, one project by the National 863 Plan, two projects supported by the National Natural Science Foundation, and 14 projects supported by the National Science Foundation of Jilin Province. She has completed over 40 research projects in total. She has authored or co-authored over 86 papers. She has obtained 30 national invention patents. She recieved the National Invention Patent Excellence Award, the Jilin Province Patent Excellence Award, and the Pittsburgh International Invention Exhibition Invention Award. She was a recipient of the Jilin Province Science and Technology Progress Award and of the first, second, and third prizes of the Science and Technology Award of CHTS. She also serves as the Expert of Youth Thousand Plans, the Evaluation Expert of the Central Organization Department outstanding Scientific and Technical Personnel, and the Expert of National 863 Plans.

NINGGUO QIAO received the B.S. degree in transportation from Shandong Jiaotong University, Jinan, China, in 2012. She is currently pursuing the Ph.D. degree with the Transportation College, Jilin University, Changchun, China. Her research mainly engaged in intelligent detection and diagnosis.

CONGCONG ZHAO received the B.S. degree in mechanical engineering from Jiangsu University, China, and the M.S. and Ph.D. degrees in automobile application engineering from Jilin University, Changchun, China, in 2016. She is currently an Associate Professor with the College of Engineering and Technology, Jilin Agricultural University, Changchun.

JIAOJIAO ZHUANG received the B.S. degree in transportation from Liaocheng University, Liaocheng, China, in 2014. She is currently pursuing the Ph.D. degree with the Transportation College, Jilin University, Changchun, China. Her research mainly engaged in intelligent detection and diagnosis.